Direct and label-free quantification of micro-RNA-181a at attomolar level in complex media using a nanophotonic biosensor

César S. Huertas,[1] David Fariña,[1] and Laura M. Lechuga[1]*

[1]Nanobiosensors and Bioanalytical Applications Group, Catalan Institute of Nanoscience and Nanotechnology (ICN2), CSIC and The Barcelona Institute of Science and Technology, CIBER-BBN, Campus UAB, Bellaterra, 08193 Barcelona, Spain

KEYWORDS: *Nanophotonic biosensor, waveguide interferometer, microRNA, miRNA, biomarker, diagnosis, cancer*

ABSTRACT: Micro-RNA signatures have emerged as advantageous biomarkers for disease prediction opening the route for the development of more direct and accurate therapies. There is an urgent need for reliable tools which can offer a fast, highly sensitive and selective detection of multiple miRNAs in complex matrices as opposed to the conventional techniques. Here, we demonstrate a nanophotonic biosensor with potential multiplexing capabilities based on interferometric bimodal nanowaveguides (BiMW) for ultra-sensitive detection of microRNAs in complex media. Concretely, the BiMW biosensor has been employed for the detection and quantification of miR-181a at attomolar concentrations (LOD = 23 aM) directly, and for the first time, in human urine samples of bladder cancer patients with no need for prior sample purification or amplification steps. We demonstrate the extremely selectivity of our methodology for miR-181a detection showing the discrimination of homologous sequences at single nucleotide mismatch and its pre-miRNA. A significant overexpression of miR-181a in bladder cancer patients was appreciated when compared with healthy controls, suggesting the implication of this miRNA in bladder cancer. Our results show that the BiMW biosensor can be used as an ultrasensitive and specific diagnostic tools by the early and fast detection and quantification of microRNAs for the prediction of diseases (as cancer) with well-defined microRNA signatures.

Mature microRNAs (miRNAs) are small and single-stranded non-coding RNAs typically containing ~19-23 nucleotides.[1] These short, endogenously expressed molecules are evolutionally conserved and they are present in a broad range of animals, plants, and viruses.[2] They play important roles in modulating several biological functions. Even though the understanding of their complex roles is not fully characterized, expression levels of specific miRNAs in tissues have already been correlated with cell fate decisions and outcome of serious disorders.[3]

The establishment of miRNA-pattern panels with diagnosis value is gaining more and more interest. It can provide detailed information of the presence of specific miRNAs which can determine the type of cancer and its stage of development (early or late stage, metastasis…). Genome-wide profiling has shown that miRNA expression signatures (miRNome) allow to discriminate with a high grade of accuracy different types of cancer[4] and to identify the tissue of origin of poorly differentiated tumors.[5] miRNAs are more stable than long mRNAs due to their small size, permitting expression profiling from fixed tissues or other biological material like blood (whole blood, plasma or serum),[6] circulating exosomes,[7] urine,[8] saliva[9] or even sputum.[10] This supports their possible use as novel, minimally invasive and robust biomarkers. Their profiling has shown to reflect the patterns observed in tumor tissues, suggesting their use as easily detectable tumor biomarkers for early diagnosis.[11] Moreover, miRNAs can be used in gene therapy for reestablishing genetic disorders.[12, 13]

Efficient and reliable detection strategies are of urgent need toward understanding the functions of miRNAs in regulatory pathways. They can bring on the development of extremely accurate diagnostic tools and miRNA-based therapies at molecular level.[14] Using miRNAs as analytical indicators holds many advantages over the traditional protein biomarkers since there are far fewer miRNAs species as compared to proteins.[15] Northern blot and reverse-transcription real-time polymerase chain reaction (RT-qPCR) techniques are considered the benchmark methods for miRNA detection.[16, 17] Several novel miRNAs have been identified by Northern blotting analyses.[17] However, this method has a poor sensitivity requiring large amounts of sample input and is relatively time-consuming. On the other hand, although RT-qPCR can cover a broad dynamic range of miRNA concentrations with a relatively high sensitivity, it requires highly purified samples. The lack of standardized protocols for miRNA extraction can introduce a high variability, leading to inaccurate analyses. In addition to these methods, microarray technology has been applied to the parallel detection of multiple miRNAs.[18] However, the complexity of miRNA labeling and narrow dynamic range of miRNA microarrays together with the difficulties for standardization limit their routine use in centralized laboratories. Next generation sequencing technology (NGS) has emerged as the preferred platform for studying miRNA expression since it allows to pool and sequence multiple samples in one lane of a sequencer.[19] However, it can be influenced by sequencing errors and often requires extensive computational analysis.

Accurate and reliable quantification of miRNAs still remains a challenging task. Only a small fraction of the mass in total RNA samples (~0.01%)[14] represents miRNA content and their expression levels can vary by as much as four orders of magnitude, requiring techniques with a wide dynamic range. Another issue is the sequence similarity among some miRNA-family members whose presence may distort the final analysis. Taken together all these difficulties, it is clear that there is an unmet need for rapid and highly sensitive and selective miRNA analysis methods that can effectively profile miRNAs in minimal amounts of sample. Several biosensor methods have been proposed to date as alternative approaches to detect miRNAs for disease diagnosis.[14, 20] In particular, optical biosensors are promising tools for the detection of miRNAs due to the advantages of preamplification-free analysis, limit of detection (LOD) at the femtomolar-attomolar (fM-aM) range, short time-to-results, multiplexing capability, and minimal sample preparation requirement, thus avoiding the introduction of measurement bias.

Different approaches based on optical biosensors for label-free detection of miRNAs have been proposed. In order to achieve wider dynamic ranges and appropriate sensitivity levels, these approaches have made use of amplification steps by employing specific antibodies for DNA/miRNA hybrids[21, 22] or gold nanoparticles[15, 23] to enhance the sensor signal. They have shown fast time to result and have achieved LODs in the low pM and fM concentrations. A Localized Surface Plasmon Resonance (LSPR) sensor using highly sensitive nanostructures (gold nanoprisms) achieved an ultra-sensitive detection of miRNAs at a LOD 91 aM in complex media avoiding the need for an amplification step.[24] However, this biosensor lacked real-time evaluation and required very long incubation times. Therefore, despite the advances achieved, all the above techniques have not shown a rapid detection of miRNAs with high sensitivities in a single reaction. In addition, most of them do not have multiplexing capabilities, which is a main requirement for routine clinical applications due to the limited sample obtained from patients, the low abundance of miRNAs, and the complexity of the sample composition.

Integrated interferometric biosensors constitute highly sensitive analytical platforms with a miniaturized size compatible with complementary metal-oxide-semiconductor (CMOS) fabrication processes, emerging as promising candidates for Lab-on-Chip devices. They represent an ideal platform for the direct and multiple miRNA detection during the analysis of complex samples avoiding pre- and post-amplification steps and with minimal sample input, thus saving time and resources. Recently, a novel integrated optical biosensor based on a slot waveguide Mach-Zehnder interferometer (MZI) configuration has been developed for miRNA detection.[25] It showed a rapid, accurate, and multiplexed detection of miRNAs in human urine samples in a single reaction, but its sensitivity levels (≤1nM) were too far from the required ones.

We present a highly sensitive nanophotonic biosensor for miRNA detection based on bimodal nanowaveguide interferometers (BiMW biosensor). The BiMW biosensor has been previously developed in our Group[26] and is fabricated with advanced silicon nanotechnology. It consists of a single channel waveguide interferometer whose mechanism relies on the interference of two waveguide modes of the same polarization avoiding light beam splitting and recombination. This novel interferometric arrangement has improved tolerance to fabrication variation and a smaller footprint, opening the possibility to fabricate more devices in the same area, with a consequent increased of the reproducibility and reliability of the sensing evaluations. In particular, we targeted miR-181a that represents a potential biomarker for cancer prediction due to its implication in the metabolic shift of cancerous cells.[27] Overexpression of miR-181a has been demonstrated in colon[27] and breast cancer,[28] hepatocellular carcinoma,[29] human gastric[30] and bladder cancer tissues.[31, 32] The high sensitivity of the BiMW nanobiosensor allows for the rapid detection (≤ 30 min) of miRNAs at a concentration as low as 23 aM, employing low amounts of sample input with no need for miRNA amplification. We also screened the levels of native endogenous miRNAs of different bladder cancer patients and control urine samples and analyzed the alterative expression levels of miR-181a, demonstrating the applicability of the BiMW biosensor for the routing clinical monitoring of miRNA levels for cancer prognosis, diagnosis and therapeutic follow-ups.

EXPERIMENTAL SECTION

Reagents, buffer solutions and miRNA sequences. The list of reagents, buffers and solvent used in this work and the design of miRNA sequences is provided in the Suplementary material.

BiMW biosensor. The BiMW device is fabricated at wafer level using standard microelectronic technology in Clean Room facilities. An array of 16 interferometers of 30 mm length is integrated over a chip. A scheme of the BiMW biosensor working principle is shown in Figure 1A. In brief, light from a polarized laser source (Helium-Neon, λ0= 660 nm) is first confined into a nanometric height rib waveguide (4 μm width x 1.5 nm height) designed to support a single transversal mode (150 nm thickness) (Section A). After some distance, this fundamental mode is coupled into a vertically bimodal section (300-350 nm thickness) through a step junction, i.e. a modal splitter (Section B). At the step junction, due to the abrupt increase of the height of the waveguide core, it splits in two modes, the fundamental and the first order modes. These two modes propagate until the end of the device, resulting in an intensity distribution which depends on the phase difference between the two modes accumulated along the propagation length. A sensing window is opened along the bimodal section of the waveguide (Section C), where the evanescent field is in contact with the external medium and is sensitive to variations of the refractive index of the environment. Due to the different confinement factors of the propagating modes, the first order mode is the main responsible for the sensing of changes occurring on the waveguide surface while the fundamental mode can be considered as a virtual reference. The superposition of these two modes results in an intensity distribution giving rise to an interferometric signal whose variations can be related to the amount of stimulus variation. On the sensor surface, when a biorecognition event occurs between a biorecognition layer and its concomitant target, the refractive index of the biosurface changes. This variation of the external refractive index affects the effective refractive index (*N*) of the propagating modes (TE_{00} for fundamental mode and TE_{10} for first order mode), producing a phase change (ΔΦ):

$$\Delta\Phi = 2\pi {}^{L_{SA}}/_{\lambda} (\Delta N_{TE10} - \Delta N_{TE00})$$

where L_{SA} is the length of the sensor area and λ is the working wavelength. The phase change produced is recorded by a two-section photodetector at the end of the waveguide (Figure 1A,

Section D). Finally, a developed all-optical phase modulation method based on Fourier transform deconvolution[33] is applied, modulating the interference signal to a real-time linear one, avoiding phase ambiguities (Figure 1B).

Polymeric flow cell fabrication. The flow cell employed contained Polydimethylsiloxane (PDMS) channels and is fabricated by polymer casting using a methacrylate mold. Elastomer and curing agent are mixed in a ratio 10:1 and air bubbles originating from their mixing are removed by a vacuum degas process. The mixture is cured for 1 hour at 75ºC to ensure cross-linking of the polymer. After this thermal process, the flow cell can be released from the methacrylate mold. The high hydrophobicity of the resulting PDMS channels is reduced by application of a Polyethylene glycol coating (PEG200, Sigma-Aldrich) after an ozone plasma treatment to expose functional groups on the polymer surface. Finally, PolyTetraFluoroEthylene (PTFE) tubes are inserted at each channel extremities and fixed with PDMS to avoid leakages or air insertion. The fluidic cell has four independent channels, with a volume of 15 µl each. Each fluidic channel addresses a group of four BiMW sensors on the fabricated chips.

Si_3N_4-surface cleaning, activation and biofunctionalization. Si_3N_4 surfaces undergo an accurate cleaning prior to its use. First the chips are sonicated sequentially in acetone, ethanol and water, 2 min each. The cleaning process was finished by ultrasonication of the Si_3N_4 surfaces in a 1:1 metanol/hydrochloric acid (MetOH/HCl) solution to remove other inorganic contamination. The chips are rinsed with milli-Q H_2O and dried under a N_2 stream.

After chip cleaning, a layer of active hydroxyl group was generated on the surface by UV/O_3 activation (BioForce Nanosciences, USA) and exposition to 15% nitric acid solution, revealing the oxide groups on the Si_3N_4 surface. Clean and hydroxyl-activated chips were immediately transferred in a 1% v/v APTES solution prepared in water-free toluene under an argon atmosphere for 1 hour. 0.3 % v/v of N, N-diisopropylethylamine (DIPEA) was employed to catalyze the hydrolysis reaction in the absence of water molecules. Finally, a curing step was performed at 110ºC for 1 hour. APTES-modified surfaces were reacted with 20 mM PDITC in a solution of 10% anhydrous pyridine in N, N-dimethylformamide (DMF) for 1 hour in darkness. PDITC-activated APTES monolayer were in-situ biofunctionalized by flowing a solution containing a mix of SH-T_{15}-miR181a probes and SH-PEGs CO_2H/NH_2 at a molar ratio of 1:1 in 2 µM total concentration in 0.1M Na_2CO_3 buffer at pH 9.5 at a constant flow rate of 5 µL/min.

Detection conditions. miRNA target detection was performed by the injection of 250µL of the samples over the surface of the BiMW biosensor at a 15 µL/min rate, with a subsequent hybridization with their complementary DNA probes immobilized on the sensor surface. Samples were dissolved in 5xSSC (0.75 M in NaCl, 0.075 M in sodium citrate) with several additives, such as 40% FA and 3M TMAC for enhancing specificity. Finally, target-probe interactions were disrupted by employing 35% FA freeing the probe for subsequent hybridization of the specific miRNA target (WARNING: Formamide is a known carcinogen. Carry out all steps involving pure formamide manipulation in a fume hood). Calibration curves were obtained by triplicate measurement of different dilutions from standards of known concentration. The mean and the standard deviation (SD) of each concentration were plotted versus the target concentration and a five-parameter model fitting was employed.

Urine samples. For miR-181a detection study, the urine samples were kindly provided by Dr. M. Sánchez-Carbayo et al. from Centro de Investigación Lucio Lascaray (Vitoria-Gasteiz, Spain), Universidad del País Vasco. Samples were collected from bladder cancer patients and healthy donors and stored in a volume of 500 µL at -80ºC until their use. For the analysis, samples were unfrozen and diluted 1:10 in the highly stringent hybridization buffer.

Data analysis. The data were analyzed using Origin 8.0 software (OriginLab, Northampton, MA). The experimental detection limit (LOD) was defined as the target concentration giving a ΔΦ (rad) in the hybridization signal at least three times higher than that of the standard deviation of the miRNA control signal.

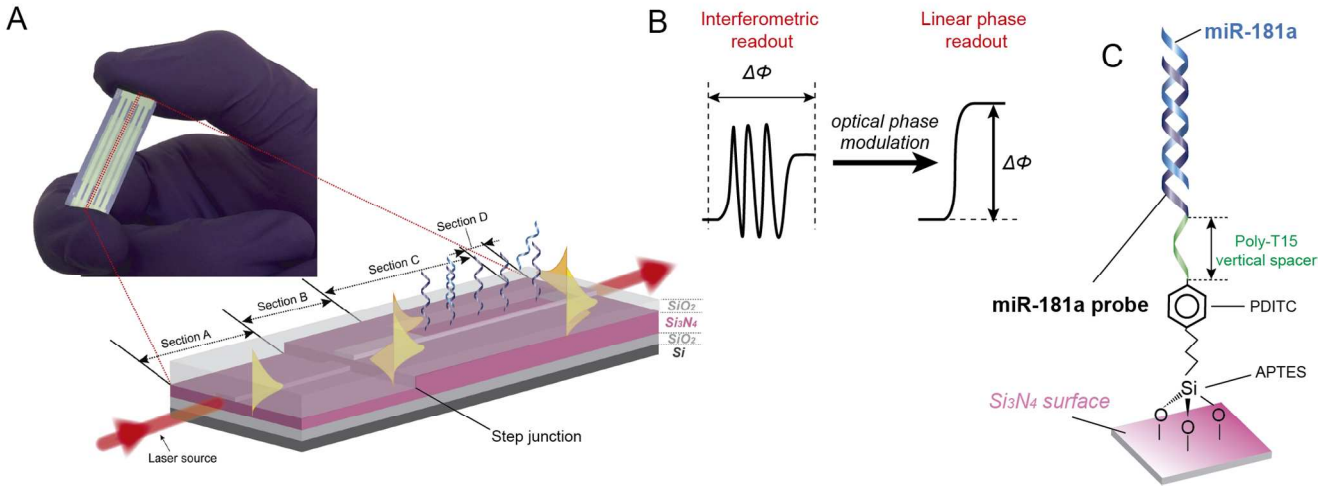

Figure 1. Photograph and working principle of a BiMW sensor chip. (A) Working principle of the BiMW interferometer: TE-polarized light is coupled in the waveguide (Section A) and propagates in its fundamental mode; it splits in two modes after the step junction (Section B) which propagate along the waveguide and generate an interferometric signal which will vary depending on whether the miR-181a hybridize or not with its specific probe at the biosensing area (Section C). (B) Optical phase modulation of the interferometric interferences. (C) Biofunctionalization strategy on the Si_3N_4 surface achieved by the generation of an APTES monolayer, activation of the amine groups through PDITC crosslinker and biofunctionalization with SH-T15-miR-181a probes via thiocarbamate bonds.

Table 1. Sequences for miR-181a probe and miRNAs synthetic targets employed for the optimization of the selective quantification of miR-181a.

Name	Sequence
miR-181a probe	5'-(SH)-(PolyT$_{15}$)-ACTCACCGACAGCGT 3'
Pre-miR-181a	5'GUGGUUGCUUCAGUGAACAUUCAACGCU GUCGGUGAGUUUGGGAUUAAAGUGAAAACCA UCGACCGUUGAUUGUACCCUCCAGCUAACCA UCC 3'
miR-181a	5'AACAUUCAACGCUGUCGGUGAGU 3'
miR-181b	5'AACAUUCAUUGCUGUCGGUGGGU 3'
miR-181c	5'AACAUUCAAC - CUGUCGGUGAGU 3'
miR-181d	5'AACAUUCAUUGUUGUCGGUGGGU 3'

RESULTS AND DISCUSSION

BiMW biosensor biofunctionalization. For a proper biofunctionalization, a suitable anchorage of the probe must be performed on the sensing area. For that, the BiMW sensor surface (Si_3N_4) was chemically modified with 3-aminopropyltriethoxy (APTES) silane, one of the most widespread used silanes in biofunctionalization processes since it generates a homogeneous monolayer under controlled conditions. This silane provides silicon surfaces with end amine groups[34, 35] that can incorporate different crosslinkers for the biofunctionalization of different biomolecules with specific chemical groups. For the APTES-monolayer activation, we employed 1,4-phenylenediisothiocyanate (PDITC) which is a small homobifunctional crosslinker commonly used in bioconjugation chemistry.[36] It has two isothiocyanate (R-NCS) groups at both ends, which are stable in solution and reactive to primary amine groups through thiourea bonds. On the other hand, R-NCS group also reacts with thiol groups, forming thiocarbamate bonds in a fast reaction.[37] The reactive capabilities and the easy management in solution of PDITC make this crosslinker very suitable for its employment for APTES-monolayer activation by thiourea bond formation. For miR-181a selective detection, we designed a single-stranded DNA probe containing the complementary sequence of miR-181a (Table 1). The DNA probe also had a sequence of 15 thymines (polyT$_{15}$), for vertical spacing, aiding the probe accessibility to the target,[38] and a functional thiol (-SH) group at the 5' end. The end thiol group serves as a reactive site for the coupling of the probes to the free R-NCS groups of the PDITC-activated APTES monolayer via thiocarbamate bonds (Figure 1C).

For DNA probe immobilization, the chip was placed in the experimental set-up and encapsulated with the fluidic cell. We injected a mixed solution of SH-T$_{15}$-miR-181a probes and SH-PEG CO_2H /NH_2 in the flow delivery system and flowed it over the sensor surface at a 5 µL/min constant rate. The PEG compounds have been demonstrated to serve as both, a surface backfiller, preventing from non-specific adsorptions, and a horizontal spacer for SH-DNA probes, aiding the control of the probe density.[39] Figure 2A shows a scheme of the functionalization process. The covalent binding of the thiolated molecules to the PDITC-activated surface was monitored in real-time by the analysis of the modulated interferometric signals of the BiMW sensor (Figure 2B). As can be appreciated, the anchorage of the probes onto the surface gave rise to a positive shift in the phase change (ΔΦ (rad) = 62.1), indicating that the DNA probe coupling through thiocarbamate bonds took place at the sensor surface.

Selective detection of miRNA-181a at attomolar level with the BiMW biosensor. To demonstrate the proper performance of the miRNA BiMW biosensor, we tested the selective detection of miR-181a. MiR-181a belongs to the miR-181 family which includes four highly conserved mature miRNAs (miR-181a, b, c, and d) derived independently from six precursors located on three different chromosomes. The four members of the human miR-181 family contain similar sequences that differ only in one to four nucleotides (Table 1). Although all members preserve the same seed sequence, they have in many cases distinct gene targets as in the case of leukemia inhibitory factor, which is targeted by miR-181d but not by miR181a.[40] In addition, while miR-181a and miR-181c encode almost identical mature miRNAs, the strength and functional specificity of these miRNAs may be modulated through their pre-miRNA loop nucleotides and/or by additional post-transcriptional processes.[41, 42] This highlights the non-redundant role of miR-181 family members and adds a potential new level of complexity for their role in cancer development, which makes mandatory the specific differentiation of these family members in order to establish a reliable diagnostic tool.

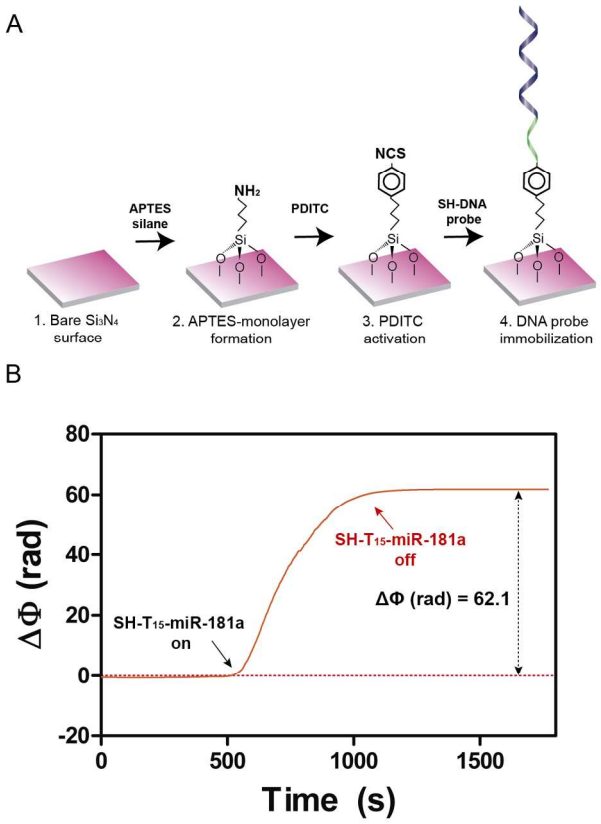

Figure 2. Biofunctionalization of the BiMW sensor surface. (A) Scheme of the functionalization process performed for miRNA detection. (B) Real-time biMW response to the immobilization of the SH-T15-miR181a probe and SH-PEG CO_2H/NH_2 mix over a PDITC-activated APTES monolayer (step 4). The sensogram shows the interaction of the injected solution with the PDITC-activated APTES monolayer (SH-T$_{15}$-miR-181a on) reaching the equilibrium (SH-T$_{15}$-miR-181a off) and giving rise to a notable increment of the phase-modulated signal.

Furthermore, the methodology should have a high capability to discriminate the pre- and mature miRNA to elucidate miRNA function and to facilitate the translation of miRNA detection method into the clinical practice.

To guarantee the specific detection of miR-181a and its homologous discrimination, we employed a hybridization buffer containing certain additives as formamide (FA) and tetramethylamonium chloride (TMAC) in 5x SSC buffer solution (i.e. 5x SSC/ FA40%/ 3M TMAC). These additives provide highly stringent conditions in order to prevent from non-desirable cross-hybridizations from the homologous miRNAs. Concretely, a high percentage of FA has been demonstrated to have a remarkably positive effect in the hybridization efficiency and discrimination of homologous sequences.[43] TMAC has been reported to be an isostabilizing agent, altering the melting temperature and making the hybridization solely dependent on oligonucleotide length independently of their GC content.[44, 45, 46]

We studied the effect of such compounds individually and their combinatorial effect employing a Surface Plasmon Resonance (SPR) biosensor since it is a well-established technique for label-free analyses (see Supporting Information). We demonstrated their discriminating effect over non-fully complementary sequences and we observed a notorious enhancement in the hybridization efficiency on the fully complementary sequences (Figure S2 and S3). Therefore, we tested the selectivity in the BiMW biosensor under these conditions by monitoring the biosensor response after the injection of the different homologous as well as the pre-miR-181a at a 100 pM concentration. As can be appreciated in the sensogram depicted in Figure 3A, all non-specific sequences returned to the baseline after the replacement with the running buffer while miR-181a produced a clearly appreciable positive shift in the biosensor response ($\Delta\Phi$ (rad) = 2.8), confirming the selective detection of miR-181a and the total discrimination of the homologous sequences.

Once we demonstrated the selectivity of the BiMW biosensor for miR-181a, we assessed its sensitivity. For that purpose, we performed a calibration curve for the direct analysis of miR-181a in the highly stringent buffer conditions previously employed. We injected in the BiMW biosensor different concentrations of miR-181a from standard solutions, covering a wide range of concentrations, from 10 aM to 10 nM. For all the concentration tested, an increase in the signal in a concentration dependent manner was detected by the formation of double-stranded DNA/miRNA heteroduplexes. The BiMW response to the range of concentrations of the synthetic miRNAs was fitted to a five-parameter logistic function.[47] As can be observed in Figure 3C, the BiMW device was able to clearly detect a wide range of miR-181a concentrations in the aM-pM range, achieving an ultra-low LoD of only 23 aM. The theoretical limit of quantification (LOQ) calculated was 79 aM, which is in close agreement with the minimum concentration measured (100 aM). The curve covered a wide range of concentrations reaching its saturating signal at concentrations equal or higher to 10 pM. Concentration-response calibration curve showed a good fitting (R^2 = 0.99) in the range of concentrations evaluated, which is advantageous for the real-time detection of miRNAs having wide-ranged expression profiles in the different stages during cancer development. The obtained LOD was 1000 million times more sensitive than the one achieved with the previously published multiplexed MZI biosensor[25] and more than four times better than the one obtained for the miRNA LSPR-based detection (92 aM).[24] In addition, our biosensor was capable to clearly monitor in real-time miR-181a interactions at concentrations as low as 100 aM directly without pre- or post- amplification processes (Figure 3B).

MiRNA-181 analysis in urine samples. In order to demonstrate the capabilities of our biosensor for real analysis, the next step was the evaluation of human samples. As previously described, miR-181a is involved in the development and proliferation of various cancers and its overexpression has been demonstrated in both circulating biofluids and tumor tissues. Among the different cancer types, we selected bladder cancer for a preliminary evaluation of the biosensor strategy as a rapid and non-invasive diagnostic tool. Bladder cancer is the fifth most common malignancy occurring worldwide and a major cause of cancer morbidity and mortality.[48] Current standard methods used to detect and monitor bladder cancer are invasive or have low sensitivity. Cytoscopy and cytology are the standard methods normally employed in bladder cancer diagnosis. The former one has a high sensitivity, but constitute an invasive technique, while the latter one is non-invasive but lacks sensitivity, especially for low-grade disease.[49] These limitations have prompted the search for more reliable non-invasive tools. For example, an accurate urinary test to detect bladder cancer would improve patient quality of life and outcome. Currently, less-invasive methods based in various urine tests have been commercialized but even though most of them are more sensitive, urine cytology continues to be more specific. Using microRNA profiling in urine samples to develop a non-invasive test for bladder cancer is of high interest. In addition, their stability in human urine supports their biomarker potential.[50] MiRNA screening in urine has demonstrated detectable miRNA species and differences in the miRNA spectra suggests the possibility that changes in the miRNA composition in urine can be used to identify physiopathological conditions.[50, 51]

We attempted the analysis of miR-181a in real human urine samples. To ensure the anti-fouling properties of the receptor monolayer, miR-181a spike-in urine samples from healthy individual were first tested over the BiMW interferometer modified only with a 100% SH-PEG CO_2H /NH_2 at a 1 μM concentration. Such monolayer would help to assess possible nonspecific adsorptions of urine matrix components, which may lead to false positive. We also analyzed the response of the monolayer containing the complementary probe for miR-181a.

The samples were diluted 1:1 in the highly selective hybridization buffer and spiked-in with miR-181a before their injection in the flow delivery system. Variations in BiMW response were monitored in real time. As can be appreciated in Figure 4A, the control receptor monolayer did not show any increment in the sensor signal at the equilibrium after the injection of the urine sample. On the other hand, an increment of $\Delta\Phi$ (πrad) = 1.69 was appreciated in the monolayer modified with the specific probe for miR-181a.

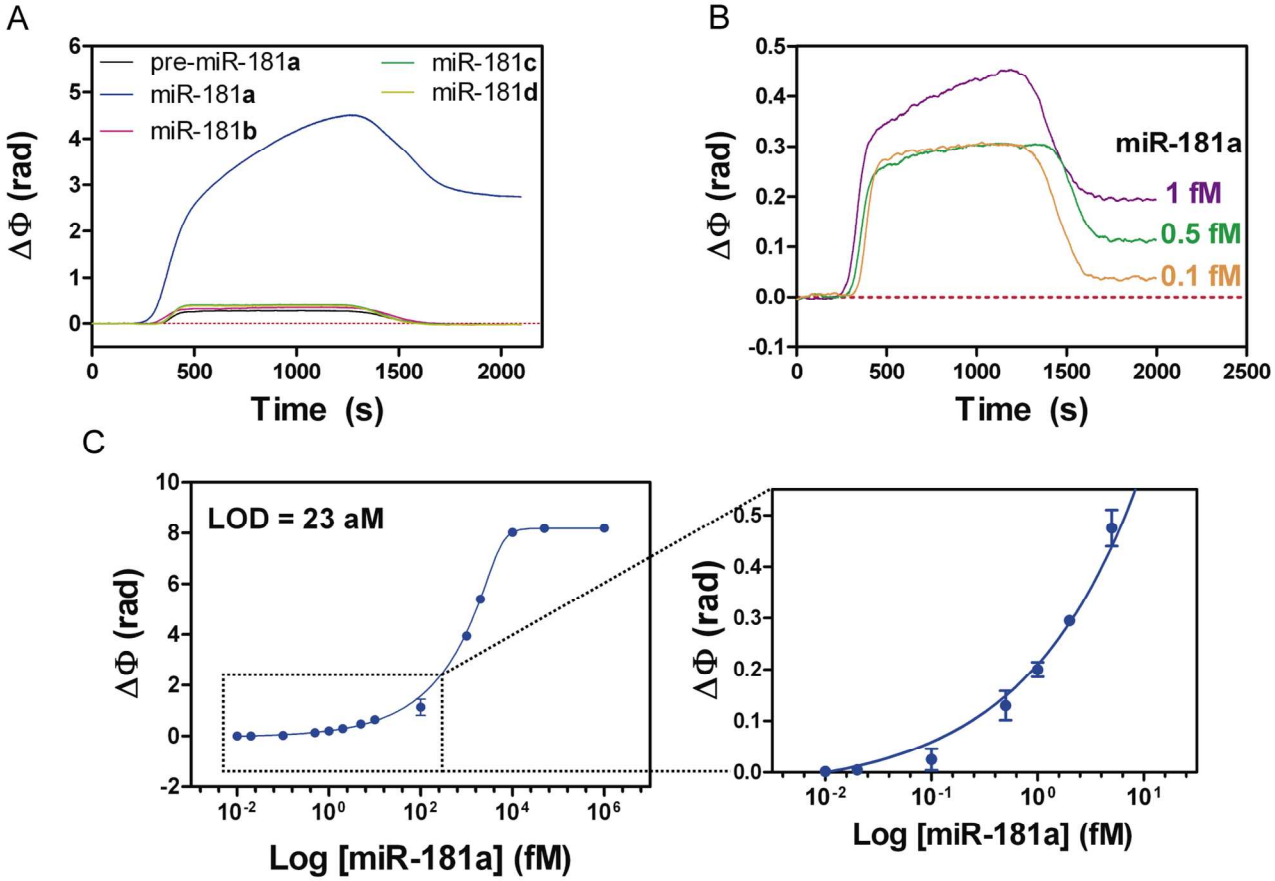

Figure 3. Detection of miR-181a by the BiMW biosensor biofunctionalized with a mix of SH-T_{15}-miR181a probes and SH-PEGs CO_2H/NH_2 at a molar ratio of 1:1 in 2 μM total concentration. (A) BiMW sensogram showing the specific detection of miR-181a (blue line) and discrimination of pre-miR-181a (black) and its homologous miRNAs 181b (purple), 181c (green) and 181d (yellow) at 100 pM concentration. (B) Sensograms obtained for the lowest concentration evaluated with the BiMW biosensor (0.1, 0.5 and 1 fM). (C) Calibration curve obtained for different concentrations of miR-181a standard solutions (10 aM- 10 nM) in semi-log scale. Solid blue line corresponds to the exponential fit of the calibration curve (R^2 = 0.99). All data show mean ± standard deviation (SD) of triplicate measurements.

These results confirmed that the methodology was highly specific toward the target miRNA and manifested that, in case we obtained a positive signal in the BiMW biosensor, it would presumably come from the specific hybridization of miR-181a to the probe at the biosensor surface.

To study the different expression of miR-181a in bladder cancer, we analyzed four urine clinical samples from both healthy donors (S1 and S2) and bladder cancer patients (S3 and S4). Urine samples were diluted 1:10 with the hybridization buffer to avoid possible saturating signals and to perform a more accurate analysis, and flowed over the biosensor surface. The signals were monitored in real time and converted into the corresponding concentrations using the calibration curve derived for miR-181a and corrected by the applied dilution factor (Figure 4B). Both healthy donors showed similar miR-181a expression (0.63 and 0.58 pM for S1 and S2, respectively). BiMW biosensor results indicated that miR-181a levels were higher in bladder cancer patients (15.1 and 18.3 pM for S3 and S4, respectively) compared to healthy control subjects, showing a 28 fold-change. These results indicated a clearly different expression of miR-181a between healthy individuals and bladder cancer patients, which suggested a possible direct implication of such miRNA in the onset of this malignancy. The miRNA can be quantified with high accuracy using the BiMW biosensor in a wide range of concentrations without the need of any modification, amplification, or labeling.

CONCLUSIONS

We have demonstrated the efficiency and ultra-sensitivity of the BiMW biosensor for the quantitative detection of cancer-associated miRNAs directly in human fluids. Concretely, we have applied it for the detection of miR-181a, a promising biomarker for cancer diagnosis due to its implication in the metabolism shift in cancerous cells. This miRNA BiMW biosensor, with a LOD of 23 aM, represents the most sensitive approach for miRNA detection so far described in a direct detection and quantification of miRNA levels without amplification or labeling steps. Discrimination between the different homologous and pre-miRNA of miR-181a has been achieved in a wide dynamic range of concentrations (aM-pM). Moreover, the BiMW analysis of human urine samples showed overexpression of miR-181a in bladder cancer patients as compared to control individuals, suggesting for the first time the direct implication of this miRNA in the outcome of this specific cancer. Further studies should be performed to confirm the implication of miR-181a in bladder cancer through metabolic shift and to establish a proper cut-off for the early determination of cancer onset.

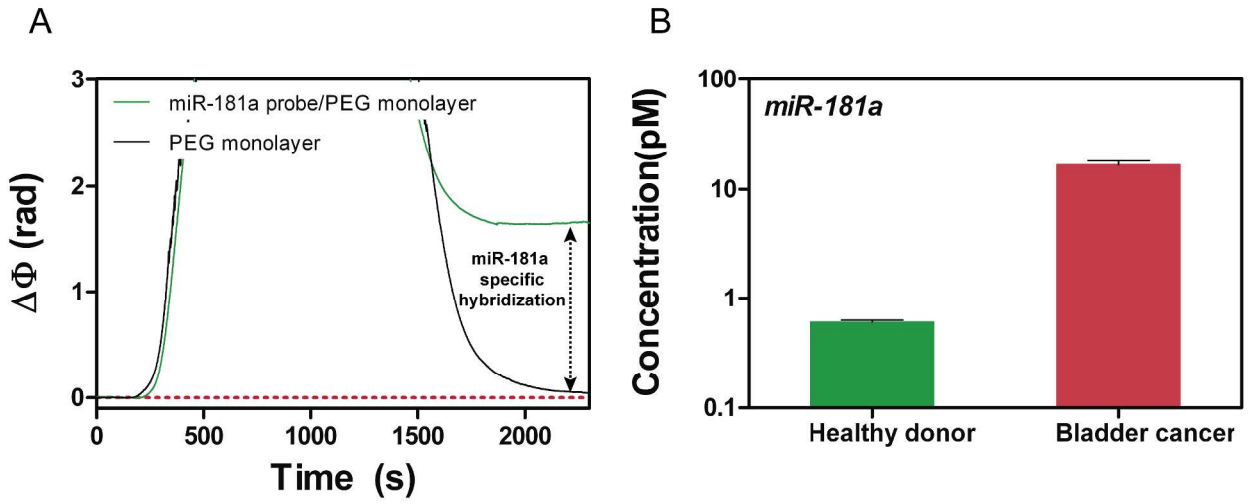

Figure 4. Analysis of miR-181a in human urine samples in the BiMW biosensor biofunctionalized with a mix of SH-T_{15}-miR181a probes and SH-PEGs CO_2H/NH_2 at a molar ratio of 1:1 in 2 μM total concentration. (A) Sensograms showing the signals of spiked-in urine samples when employing the anti-fouling monolayer with the specific miR-181a probe (green line) and a control anti-fouling monolayer (black line). (B) Concentrations of miR-181a in urine samples from healthy donors (0.6 pM) and bladder cancer patients (16.7 pM) obtained by interpolation of the BiMW biosensor signal in the calibration curve (Figure 3C).

Overall, the proposed biosensor is the first methodology reported in BiMW for nucleic acid detection with clinical purposes and constitutes an extraordinary opportunity for the development of multiplexed Lab-on-a-Chip platforms that provide simultaneous detection of specific miRNA panels in very low amounts of human fluids with ultra-high sensitivity. The implementation in Point-of-Care systems may drastically improve not only cancer diagnosis and prognosis, but also may increase treatment and curation probabilities.

ASSOCIATED CONTENT

Supporting Information

The Supporting Information is available free of charge on the ACS Publications website.

Additional text describing reagents, solvents and the sources and software employed for the design of the miRNA sequences, as well as, the Surface Plasmon Resonance biosensor and the optimization performed for miR-181a specific detection (PDF).

AUTHOR INFORMATION

Corresponding Author

*L. M. Lechuga: *laura.lechuga@cin2.es. Tel.: + 34 93 737 4620*

Author Contributions

The manuscript was written through contributions of all authors. / All authors have given approval to the final version of the manuscript.

Funding Sources

This work was financially supported by EPISENS project of the Spanish Ministry of Science and Innovation (TEC2012-3428). The nanoB2A is a consolidated research group (Grup de Recerca) of the Generalitat de Catalunya and has support from the Departament d'Universitats, Recerca i Societat de la Informació de la Generalitat de Catalunya (2014 SGR 624).

ACKNOWLEDGMENT

ICN2 acknowledges support of the Spanish MINECO through the Severo Ochoa Centers of Excellence Program under Grant SEV-2013-0295. We thank to Dr. M. Sánchez-Carbayo et al. from Centro de Investigación Lucio Lascaray (Vitoria-Gasteiz, Spain), Universidad del País Vasco, for supplying urine samples.

REFERENCES

1. Lim, L. P.; Lau, N. C.; Garrett-Engele, P.; Grimson, A.; Schelter, J. M.; Castle, J.; Bartel, D. P.; Linsley, P. S.; Johnson, J. M., Microarray analysis shows that some microRNAs downregulate large numbers of target mRNAs. *Nature* **2005,** *433* (7027), 769-773.
2. He, L.; Hannon, G. J., MicroRNAs: small RNAs with a big role in gene regulation. *Nature Reviews Genetics* **2004,** *5* (7), 522-531.
3. Iorio, M. V.; Croce, C. M., MicroRNA dysregulation in cancer: diagnostics, monitoring and therapeutics. A comprehensive review. *EMBO molecular medicine* **2012,** *4* (3), 143-159.
4. Lu, J.; Getz, G.; Miska, E. A.; Alvarez-Saavedra, E.; Lamb, J.; Peck, D.; Sweet-Cordero, A.; Ebert, B. L.; Mak, R. H.; Ferrando, A. A., MicroRNA expression profiles classify human cancers. *Nature* **2005,** *435* (7043), 834-838.
5. Rosenfeld, N.; Aharonov, R.; Meiri, E.; Rosenwald, S.; Spector, Y.; Zepeniuk, M.; Benjamin, H.; Shabes, N.; Tabak, S.; Levy, A., MicroRNAs accurately identify cancer tissue origin. *Nature biotechnology* **2008,** *26* (4), 462-469.
6. Schwarzenbach, H.; Hoon, D. S.; Pantel, K., Cell-free nucleic acids as biomarkers in cancer patients. *Nature Reviews Cancer* **2011,** *11* (6), 426-437.
7. Taylor, D. D.; Gercel-Taylor, C., MicroRNA signatures of tumor-derived exosomes as diagnostic biomarkers of ovarian cancer. *Gynecologic oncology* **2008,** *110* (1), 13-21.
8. Hanke, M.; Hoefig, K.; Merz, H.; Feller, A. C.; Kausch, I.; Jocham, D.; Warnecke, J. M.; Sczakiel, G. In *A robust methodology to study urine microRNA as tumor marker: microRNA-126 and microRNA-182 are related to urinary bladder cancer*, Urologic Oncology: Seminars and Original Investigations, Elsevier: 2010; pp 655-661.
9. Michael, A.; Bajracharya, S. D.; Yuen, P. S.; Zhou, H.; Star, R. A.; Illei, G. G.; Alevizos, I., Exosomes from human saliva as a source of microRNA biomarkers. *Oral diseases* **2010,** *16* (1), 34-38.
10. Xie, Y.; Todd, N. W.; Liu, Z.; Zhan, M.; Fang, H.; Peng, H.; Alattar, M.; Deepak, J.; Stass, S. A.; Jiang, F., Altered miRNA expression in sputum for diagnosis of non-small cell lung cancer. *Lung cancer* **2010,** *67* (2), 170-176.
11. Heneghan, H. M.; Miller, N.; Lowery, A. J.; Sweeney, K. J.; Newell, J.; Kerin, M. J., Circulating microRNAs as novel minimally

invasive biomarkers for breast cancer. *Annals of surgery* **2010,** *251* (3), 499-505.
12. Bader, A. G.; Lammers, P., The therapeutic potential of microRNAs. *Innovations in Pharmaceutical Technology* **2011**, 52-55.
13. Ling, H.; Fabbri, M.; Calin, G. A., MicroRNAs and other non-coding RNAs as targets for anticancer drug development. *Nature reviews Drug discovery* **2013,** *12* (11), 847-865.
14. Dong, H.; Lei, J.; Ding, L.; Wen, Y.; Ju, H.; Zhang, X., MicroRNA: function, detection, and bioanalysis. *Chemical reviews* **2013,** *113* (8), 6207-6233.
15. Vaisocherová, H.; Šípová, H.; Víšová, I.; Bocková, M.; Špringer, T.; Ermini, M. L.; Song, X.; Krejčík, Z.; Chrastinová, L.; Pastva, O., Rapid and sensitive detection of multiple microRNAs in cell lysate by low-fouling surface plasmon resonance biosensor. *Biosensors and Bioelectronics* **2015,** *70*, 226-231.
16. Benes, V.; Castoldi, M., Expression profiling of microRNA using real-time quantitative PCR, how to use it and what is available. *Methods* **2010,** *50* (4), 244-249.
17. Lagos-Quintana, M.; Rauhut, R.; Yalcin, A.; Meyer, J.; Lendeckel, W.; Tuschl, T., Identification of tissue-specific microRNAs from mouse. *Current Biology* **2002,** *12* (9), 735-739.
18. Thomson, J. M.; Parker, J.; Perou, C. M.; Hammond, S. M., A custom microarray platform for analysis of microRNA gene expression. *Nature methods* **2004,** *1* (1), 47-53.
19. Eminaga, S.; Christodoulou, D. C.; Vigneault, F.; Church, G. M.; Seidman, J. G., Quantification of microRNA Expression with Next-Generation Sequencing. *Current Protocols in Molecular Biology* **2013**, 4.17. 1-4.17. 14.
20. Hamidi-Asl, E.; Palchetti, I.; Hasheminejad, E.; Mascini, M., A review on the electrochemical biosensors for determination of microRNAs. *Talanta* **2013,** *115*, 74-83.
21. Sipova, H.; Zhang, S.; Dudley, A. M.; Galas, D.; Wang, K.; Homola, J., Surface Plasmon Resonance Biosensor for Rapid Label-Free Detection of Microribonucleic Acid at Subfemtomole Level *Analytical Chemistry Article ASAP* **2010,** *82* (24), 10110-10115.
22. Qavi, A. J.; Kindt, J. T.; Gleeson, M. A.; Bailey, R. C., Anti-DNA: RNA antibodies and silicon photonic microring resonators: increased sensitivity for multiplexed microRNA detection. *Analytical chemistry* **2011,** *83* (15), 5949-5956.
23. Wang, Q.; Li, Q.; Yang, X.; Wang, K.; Du, S.; Zhang, H.; Nie, Y., Graphene oxide–gold nanoparticles hybrids-based surface plasmon resonance for sensitive detection of microRNA. *Biosensors and Bioelectronics* **2016,** *77*, 1001-1007.
24. Joshi, G. K.; Deitz-McElyea, S.; Liyanage, T.; Lawrence, K.; Mali, S.; Sardar, R.; Korc, M., Label-Free Nanoplasmonic-Based Short Noncoding RNA Sensing at Attomolar Concentrations Allows for Quantitative and Highly Specific Assay of MicroRNA-10b in Biological Fluids and Circulating Exosomes. *ACS nano* **2015,** *9* (11), 11075-11089.
25. Liu, Q.; Shin, Y.; Kee, J. S.; Kim, K. W.; Rafei, S. R. M.; Perera, A. P.; Tu, X.; Lo, G.-Q.; Ricci, E.; Colombel, M., Mach–Zehnder interferometer (MZI) point-of-care system for rapid multiplexed detection of microRNAs in human urine specimens. *Biosensors and Bioelectronics* **2015,** *71*, 365-372.
26. Zinoviev, K.; Gonzalez Guerrero, A.; Dominguez, C.; Lechuga, L., Integrated Bimodal Waveguide Interferometric Biosensor for Label-Free Analysis. *Journal of Lightwave Technology* **2011,** *29* (13), 1926-1930.
27. Wei, Z.; Cui, L.; Mei, Z.; Liu, M.; Zhang, D., miR-181a mediates metabolic shift in colon cancer cells via the PTEN/AKT pathway. *FEBS letters* **2014,** *588* (9), 1773-1779.
28. Jiao, X.; Zhao, L.; Ma, M.; Bai, X.; He, M.; Yan, Y.; Wang, Y.; Chen, Q.; Zhao, X.; Zhou, M., MiR-181a enhances drug sensitivity in mitoxantone-resistant breast cancer cells by targeting breast cancer resistance protein (BCRP/ABCG2). *Breast cancer research and treatment* **2013,** *139* (3), 717-730.
29. Ji, J.; Yamashita, T.; Wang, X. W., Wnt/beta-catenin signaling activates microRNA-181 expression in hepatocellular carcinoma. *Cell Biosci* **2011,** *1* (4), 10.1186/2045-3701-1-4.
30. Zhang, X.; Nie, Y.; Du, Y.; Cao, J.; Shen, B.; Li, Y., MicroRNA-181a promotes gastric cancer by negatively regulating tumor suppressor KLF6. *Tumor Biology* **2012,** *33* (5), 1589-1597.
31. Puzio-Kuter, A. M.; Castillo-Martin, M.; Kinkade, C. W.; Wang, X.; Shen, T. H.; Matos, T.; Shen, M. M.; Cordon-Cardo, C.; Abate-Shen, C., Inactivation of p53 and Pten promotes invasive bladder cancer. *Genes & development* **2009,** *23* (6), 675-680.
32. Song, T.; Xia, W.; Shao, N.; Zhang, X.; Wang, C.; Wu, Y.; Dong, J.; Cai, W.; Li, H., Differential miRNA expression profiles in bladder urothelial carcinomas. *Asian Pac J Cancer Prev* **2010,** *11* (4), 905-911.
33. Dante, S.; Duval, D.; Sepúlveda, B.; González-Guerrero, A. B.; Sendra, J. R.; Lechuga, L. M., All-optical phase modulation for integrated interferometric biosensors. *Optics express* **2012,** *20* (7), 7195-7205.
34. Diao, J.; Ren, D.; Engstrom, J. R.; Lee, K. H., A surface modification strategy on silicon nitride for developing biosensors. *Analytical biochemistry* **2005,** *343* (2), 322-328.
35. Fernandez, R. E.; Bhattacharya, E.; Chadha, A., Covalent immobilization of Pseudomonas cepacia lipase on semiconducting materials. *Applied Surface Science* **2008,** *254* (15), 4512-4519.
36. Manning, M.; Harvey, S.; Galvin, P.; Redmond, G., A versatile multi-platform biochip surface attachment chemistry. *Materials Science and Engineering: C* **2003,** *23* (3), 347-351.
37. Gokmen, M. T.; Brassinne, J.; Prasath, R. A.; Du Prez, F. E., Revealing the nature of thio-click reactions on the solid phase. *Chemical Communications* **2011,** *47* (16), 4652-4654.
38. Steel, A. B.; Levicky, R. L.; Herne, T. M.; Tarlov, M. J., Immobilization of nucleic acids at solid surfaces: effect of oligonucleotide length on layer assembly. *Biophysical journal* **2000,** *79* (2), 975-981.
39. Joshi, G. K.; Deitz-McElyea, S.; Johnson, M.; Mali, S.; Korc, M.; Sardar, R., Highly specific plasmonic biosensors for ultrasensitive microRNA detection in plasma from pancreatic cancer patients. *Nano letters* **2014,** *14* (12), 6955-6963.
40. Belkaya, S.; Silge, R. L.; Hoover, A. R.; Medeiros, J. J.; Eitson, J. L.; Becker, A. M.; de la Morena, M. T.; Bassel-Duby, R. S.; van Oers, N., Dynamic modulation of thymic microRNAs in response to stress. *PloS one* **2011,** *6* (11), e27580.
41. Kuchen, S.; Resch, W.; Yamane, A.; Kuo, N.; Li, Z.; Chakraborty, T.; Wei, L.; Laurence, A.; Yasuda, T.; Peng, S., Regulation of microRNA expression and abundance during lymphopoiesis. *Immunity* **2010,** *32* (6), 828-839.
42. Liu, G.; Min, H.; Yue, S.; Chen, C.-Z., Pre-miRNA loop nucleotides control the distinct activities of mir-181a-1 and mir-181c in early T cell development. *PloS one* **2008,** *3* (10), e3592-e3592.
43. Huertas, C. S.; Carrascosa, L.; Bonnal, S.; Valcárcel, J.; Lechuga, L., Quantitative evaluation of alternatively spliced mRNA isoforms by label-free real-time plasmonic sensing. *Biosensors and Bioelectronics* **2016,** *78*, 118-125.
44. Duby, A.; Jacobs, K. A.; Celeste, A., Using synthetic oligonucleotides as probes. *Current Protocols in Molecular Biology* **2001**, 6.4. 1-6.4. 10.
45. Napolitano, N. M.; Rohlfs, E. M.; Heim, R. A., Simultaneous Detection of Multiple Point Mutations Using Allele-Specific Oligonucleotides. *Current Protocols in Human Genetics* **2004**, 9.4. 1-9.4. 10.
46. Schwinefus, J. J.; Kuprian, M. J.; Lamppa, J. W.; Merker, W. E.; Dorn, K. N.; Muth, G. W., Human telomerase RNA pseudoknot and hairpin thermal stability with glycine betaine and urea: Preferential interactions with RNA secondary and tertiary structures. *Biochemistry* **2007,** *46* (31), 9068-9079.
47. Giraldo, J.; Vivas, N. M.; Vila, E.; Badia, A., Assessing the (a) symmetry of concentration-effect curves: empirical versus mechanistic models. *Pharmacology & therapeutics* **2002,** *95* (1), 21-45.
48. Jemal, A.; Murray, T.; Ward, E.; Samuels, A.; Tiwari, R. C.; Ghafoor, A.; Feuer, E. J.; Thun, M. J., Cancer statistics, 2005. *CA: a cancer journal for clinicians* **2005,** *55* (1), 10-30.
49. Mengual, L.; Lozano, J. J.; Ingelmo-Torres, M.; Gazquez, C.; Ribal, M. J.; Alcaraz, A., Using microRNA profiling in urine samples to develop a non-invasive test for bladder cancer. *International Journal of Cancer* **2013,** *133* (11), 2631-2641.
50. Mall, C.; Rocke, D. M.; Durbin-Johnson, B.; Weiss, R. H., Stability of miRNA in human urine supports its biomarker potential. *Biomarkers in medicine* **2013,** *7* (4), 623-631.
51. Weber, J. A.; Baxter, D. H.; Zhang, S.; Huang, D. Y.; Huang, K. H.; Lee, M. J.; Galas, D. J.; Wang, K., The microRNA spectrum in 12 body fluids. *Clinical chemistry* **2010,** *56* (11), 1733-1741.

For TOC only

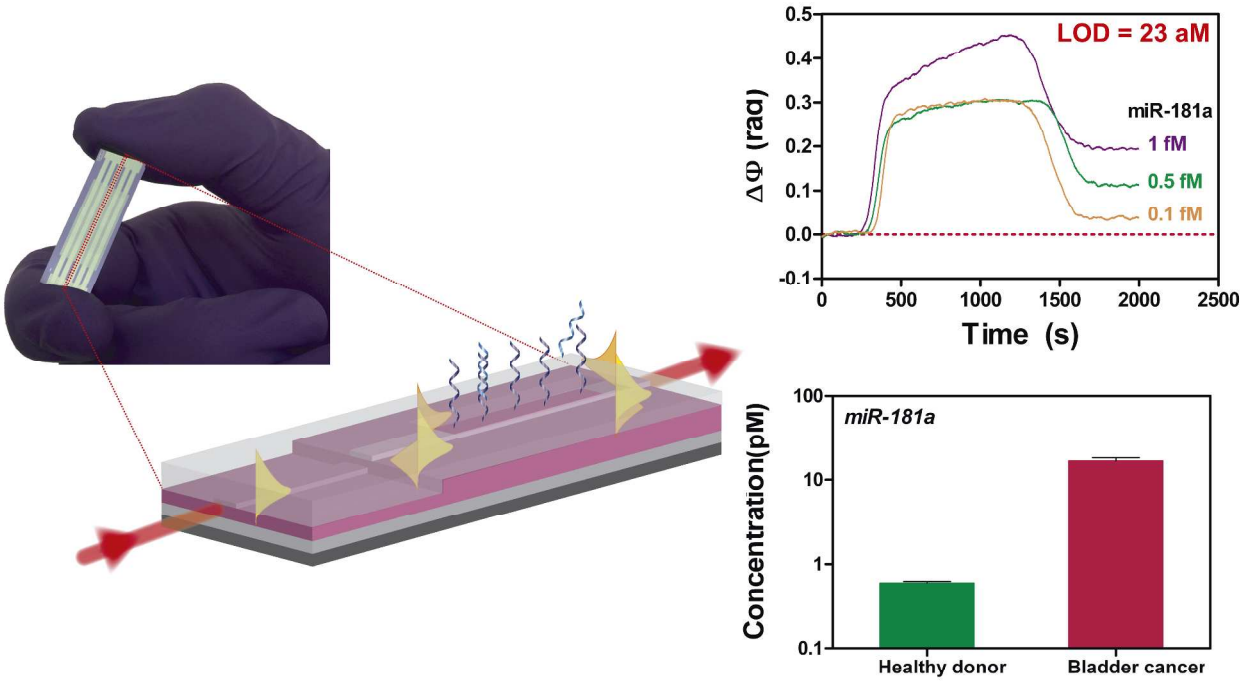
LOD = 23 aM
miR-181a
1 fM
0.5 fM
0.1 fM
ΔΦ (rad)
Time (s)
miR-181a
Concentration(pM)
Healthy donor
Bladder cancer